Research Article
doi.org/10.1002/cplu.202200411

Chemistry Europe
European Chemical Societies Publishing

www.chempluschem.org

Tris(β-ketoiminate) Aluminium(III) Compounds as Aluminium Oxide Precursors

Samuel P. Douglas[+], Erica N. Faria[+], Shreya Mrig, Ye Zhou, Leonardo Santoni, Adam J. Clancy, and Caroline E. Knapp*[a]

Precursor design is the crucial step in tailoring the deposition profile towards a multitude of functional materials. Most commercially available aluminium oxide precursors require high processing temperatures (>500 °C). Herein, we report the tuning of the decomposition profile (200–350 °C) of a range of octahedrally coordinated tris(β-ketoiminate) aluminium complexes of the type [Al(MeCN(R)CHC=OMe)$_3$], by varying the R substituents in the ligands. The complexes are derived from the reaction of trimethylamine alane (TMAA) and a series of N-substituted β-ketoiminate ligands (R-acnacH, R = Me, Et, ^{i}Pr, Ph) with varying R-substituents sizes. When the more sterically encumbered ligand (R = Mes) was used, the Al atom became five-coordinate, therefore representing the threshold to octahedral coordination around the metal in these type of compounds, which, consequently, lead to a change of decomposition profile. The resulting compounds have been characterised by NMR spectroscopy, mass spectrometry, elemental analysis and single crystal X-ray diffraction. [Al(MeCN(Me)CHC=OMe)$_3$] has been used as a single source precursor for the deposition of Al_2O_3. Thin films were deposited *via* aerosol assisted chemical vapour deposition (AACVD), with toluene as the solvent, and were analysed using SEM, EDX and XPS.

Introduction

Chelating ligands are well established in the field of metal-organic chemistry.[1–3] Among these ligands, conjugated six-membered ring chelates such as β-diketonates or "acacs" and β-ketoiminates or "acnacs" have been widely used (Figure 1). Each motif can also exist as the protonated, uncomplexed, organic compound (β-diketone and β-ketoimine, respectively). There has been particular interest in these ligand systems for use as precursors over the last few decades, especially in the field of microelectronics, where techniques such as metal-organic chemical vapour deposition (MOCVD) and atomic layer deposition (ALD) have been used to deposit thin films of metal-based functional materials.[4–8]

Group 13 β-diketonates are a well-known family of compounds, existing as *tris* ligated systems when no other types of ligands are present. Aluminium acetylacetonate, [Al(acac)$_3$], is an example of such compounds and has a rich history as a precursor for the deposition of aluminium oxides films through MOCVD.[9–13]

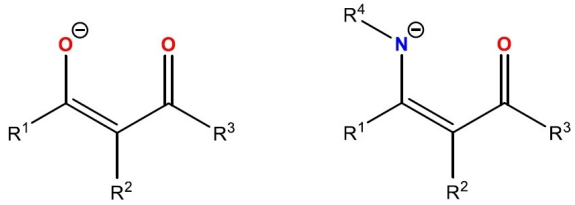

Figure 1. (a) β-Diketonate and (b) β-ketoiminate chelating ligands.

Despite the great historic interest in β-diketone ligands (Figure 1a), the lack of opportunity to functionalise them closer to the metal binding site limits their use, as there are fewer opportunities to tailor the properties of the resultant metal complex through this ligand. To overcome this issue, the closely related β-ketoimine ligand can be used instead (Figure 1b).[14–18] They are most commonly synthesised by the condensation reaction of a β-diketone with a primary amine in the presence of a catalytic acid. Functionalization at the enamine group can drastically change the resultant properties of the ligand and, hence, of the metal complex. Many variations of β-ketoimine compounds have been prepared, including examples containing alkyl,[19] aryl[20] and silyl[21] R groups. There are also known examples of β-ketoimine compounds where the careful choice of the R group leads to ligand systems with a greater denticity than two.[22,23]

As with β-diketones, all Al complexes containing β-ketoiminates ligands feature Al(III). Interestingly, *mono*- and *bis*-ligated systems using these ligands are much more common than the β-diketonates, with the prevalence of heteroleptic structures being much greater. Despite there being several *mono* and *bis* ligated systems featuring alkyl,[24] alkoxide[25] and halide[24] co-ligands, only one example of an aluminium compound featuring β-ketoimine and hydride ligands exists.[8]

[a] *Dr. S. P. Douglas,[+] Dr. E. N. Faria,[+] S. Mrig, Y. Zhou, Dr. A. J. Clancy, Dr. C. E. Knapp*
Department of Chemistry
University College London
20 Gordon Street
WC1H 0AJ London (UK)
E-mail: caroline.knapp@ucl.ac.uk

[+] *These authors contributed equally to this work.*

Supporting information for this article is available on the WWW under https://doi.org/10.1002/cplu.202200411

Tris(β-ketoiminate) aluminium complexes do exist, although are much rarer than with β-diketonate ligands. Only three complexes of this kind are reported in the literature, all containing aryl N-substituents.[20,26,27] The first one was synthesised by Altaf *et al.*,[26] who produced an octahedral Al(III) tris(β-ketoiminate) complex using a β-ketoiminate ligand with a 4-*tert*butylphenyl N-substituent.[26] The second was synthesised by Olejník *et al.* using a methoxyaryl N-substituent[27], and the third tris(β-ketoiminate) octahedral Al complex was reported by Jana *et al.*,[20] who were investigating group 13 complexes containing β-ketoiminate and β-diketiminate ligands. β-Ketoiminate compounds have also been used in Al-based deposition chemistry, albeit infrequently. These compounds are more prominently used for the group 2 metals, where they have allowed the preparation of volatile monomeric compounds.[28]

Six-coordinated, octahedral, complexes containing bidentate chelating ligands can form two isomers that are mirror images of one another. They can adopt either meridional or facial configurations and can be either lambda, Λ, left-handed, or delta, Δ, right-handed. Tris-bidentate complexes tend to crystallize as racemic mixtures.

Six-membered ring chelating metal compounds have a rich history in precursor chemistry, particularly in the deposition of metal oxide films.[28–31] Examples of the use of such ligands to produce the metallic element upon deposition do exist, but are rare.[30] Much of the research in *acac* metal complexes for deposition chemistry has focused on increasing the volatility of such compounds through adding fluorinated groups and, less so, into lowering their decomposition temperatures. Regarding aluminium, [Al(acac)$_3$] and its derivatives have been investigated extensively for the deposition of Al_2O_3 thin films since the 1960s.[32] Aluminium's high affinity to oxygen implies it is highly unlikely that such precursors will be able to convert to the metallic element, even under the harshest of conditions, unlike what is seen in copper metal deposition chemistry.[30]

With an increasing demand for industrially useful materials to be more efficient, the search for precursors that decompose at lower temperatures also increases to adjust to modern lower temperature deposition techniques that can deposit metallic features onto low-cost, flexible substrates.[33] As such, a good precursor should decompose within the 50–200 °C temperature window.[33] One way to access the suitability of a metal complex as a precursor to thin films is by analysing its thermal decomposition profile.[4,34–36] The reduced number of examples of tris(β-ketoiminate) aluminium complexes described in the literature prompted us to investigate the accessibility of such compounds through ligand substitution reactions. For this purpose, the nature of the R-substituents was carefully chosen in order to explore the effect of steric bulk of the ligand on their arrangement around the metal, on the metal's coordination number as well as on the decomposition profile of the resulting compounds. The metal complexes were characterised by NMR spectroscopy, mass spectrometry, elemental analysis, with particular focus given to X-ray crystallographic structural characterisation and thermal decomposition analysis. Herein, we report the synthesis of four novel tris(β-ketoiminate) aluminium complexes containing β-ketoiminate ligands with varying R-substituent groups (Me, Et, ^{i}Pr and Mes), as well as the already known analogue containing R = Ph for means of comparison.[20]

Results and discussion

Synthesis of β-ketoimine ligands

β-Ketoimine ligands can be synthesised *via* the condensation reaction of β-diketones with primary amines. Many techniques have been used to synthesise such compounds, including the use of solid acid catalysts, catalytic amounts of iodine and microwave-assisted processes.[37–39] However, the synthesis of the β-ketoimine ligands featured in this work use the facile reaction of acetylacetone with a primary amine, either at room temperature or heated to reflux, as a simpler and most cost-effective alternative method offering good yields.[40]

The β-ketoimines N-methyl-4-amino-3-penten-2-one (**Me-acnacH**), N-ethyl-4-amino-3-penten-2-one (**Et-acnacH**), N-isopropyl-4-amino-3-penten-2-one (**^{i}Pr-acnacH**), N-phenyl-4-amino-3-penten-2-one (**Ph-acnacH**) and N-(2,4,6-trimethylphenyl)-4-amino-3-penten-2-one (**Mes-acnacH**) were selected due to their variations in steric bulk.

The formation of the β-ketoimine ligands can be easily identified by the characteristic downfield chemical shift of the broad NH proton resonance in the amine of the β-chelating compound between 11 and 12 ppm. This chemical shift occurs due to deshielding effect of the imino group intramolecularly hydrogen bonding with the adjacent carbonyl group. β-ketoimines undergo rapid proton exchange between the nitrogen and oxygen atoms and, thus, exists in two tautomeric forms that rapidly interconvert (Scheme 1).

Synthesis of tris(β-ketoiminate) aluminium complexes

Aiming to form aluminium complexes with low decomposition temperatures, β-ketoimine ligands were chosen to complex to aluminium through the reaction with trimethylamine alane, [$Me_3N{\cdot}AlH_3$] (TMAA). TMAA itself, is a precursor that can be used to deposit aluminium metallic films at low temperature, however it is extremely air and temperature sensitive and thus, more challenging and expensive to apply in industrial settings.[41–43] Through numerous reactions using different molar ratios of β-ketoimine, we concluded that, to sufficiently stabilise the aluminium atom, three equivalents of ligand were required, therefore liberating three equivalents of dihydrogen gas, which acts as the entropic driving force (Scheme 2). Sub-stoichiometric ratios of ligand gave lower yields of the tris-adducts, while

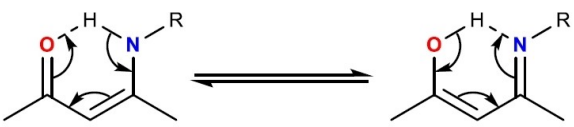

Scheme 1. Tautomeric forms (conjugation) of β-ketoimines.

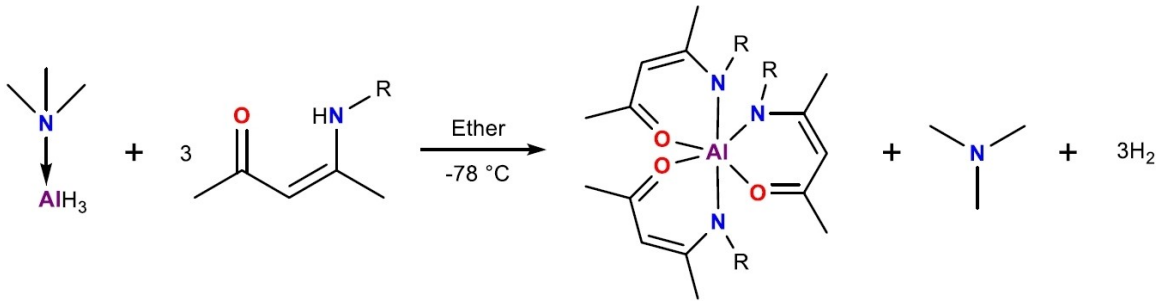

Scheme 2. General reaction for the formation of the tris(β-ketoiminate) aluminium complexes.

using excess amounts resulted in wasted reagent – mono- or bis-species could not be isolated and characterised. In addition to dihydrogen, the formation of the low boiling trimethylamine (B.P. 3 °C) as the only other by-product, allows for a more simplified purification of these complexes.

The complexes with alkyl R groups (**1**–**3**) were soluble in diethyl ether and hence were crystallized from the reaction solvent at −20 °C. Complexes with aryl groups (**4** and **5**) were not soluble in diethyl ether due to the larger hydrophobic character of the R groups and, hence, were crystallised from toluene at −20 °C.

As mentioned, there are only three other tris(β-ketoiminate) aluminium compounds in the literature, Jana's[20] phenyl, Olejník's methoxyaryl,[27] and Altaf's[26] bulkier (4-*tert*butylphenyl) complexes, with no alkyl adducts known. Other conventional *tris* coordinated aluminium complexes featuring bidentate ligands are limited to a range of tris(β-diketonate) aluminium analogues,[25,44] one tris(β-diketimine) aluminium complex,[45] as well as others that employ less comparable ligand systems, such as 8-hydroxyquinoline, that also feature a AlO_3N_3 core,[46–50] and tris-aluminium alkoxide complexes.[51–53]

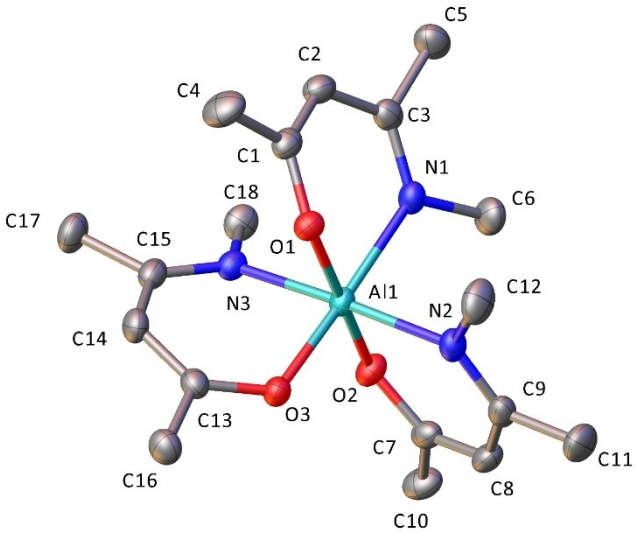

Figure 2. Molecular structure of **[Al(Me-acnac)$_3$]** (**1**). Thermal ellipsoids pictured at 50% probability. Hydrogen atoms omitted for clarity. Selected bond lengths (Å) and angles (deg): Al1–O1: 1.8769(9); Al1–O2: 1.8589(9); Al1–O3: 1.8675(9); Al1–N1: 2.0352(11); Al1–N2: 2.0331(11); Al1–N3: 2.0306(10) O1–Al1–O2: 175.27(4); O1–Al1–N1: 86.73(4); N1–Al1–O3: 174.93(4); N1–Al1–N2: 89.78(4).

[Al(MeCN(Me)CHOMe)$_3$] ([Al(Me-acnac)$_3$], 1)

Compound **1**, **[Al(Me-acnac)$_3$]**, was prepared by the σ-bond metathesis reaction of TMAA with three equivalents of Me-acnacH in diethyl ether at low temperature, with the recrystallized compound having excellent purity, as demonstrated by ^{1}H and ^{13}C{^{1}H} NMR spectra, with a moderate yield (54%). Colourless single crystals suitable for X-ray diffraction experiments were obtained from a concentrated diethyl ether solution at −20 °C and were used to determine the crystal structure of compound **1** (Figure 2).

Compound **1** crystallised in the triclinic space group $P\bar{1}$. The complex is a 1:3 monomer, with three chelating bidentate β-ketoiminate ligands, each binding *via* both O and N atoms. The OC_3N backbone of all three β-ketoiminate ligands coordinated to the Al atom, have a delocalised π-electronic system. The three ligands form an example of an octahedral arrangement around the six-coordinate Al metal, in a *mer* configuration, in order to reduce steric clash between the bulky imino groups. The distortion found in the octahedral arrangement of the ligands precludes the generation of each bidentate ligand by symmetry and, thus, although each ligand environment is chemically identical, they are crystallographically inequivalent, leading to a host of comparable, but different, bond lengths and angles. These findings are likely a result of the *mer*-configuration of the ligands around the aluminium, as well as different *cis*/*trans* heteroatom relationships. Interestingly, complex **1** crystalizes as a racemic mixture of the enantiomers delta, Δ, and lambda, Λ, as shown in ESI (section 2a).

Crystallographic data of complex **1** is consistent with the three other examples of this kind found in the literature.[20,26,27] Due to the steric constraints of the bidentate ligands, the octahedral geometry is slightly distorted, as evident by the O(1)–Al(1)–N(1) angle of 86.73(4)°, deviating from the 90° ideal angle. Distortion of other heteroatom-Al-heteroatom angles, such as O(1)–Al(1)–O(2) (175.27(4)° and N(1)–Al(1)–O(3) (174.93(4)°) angles are also observed in the structure. The Al–N–C–C–C–O six-membered chelate rings are slightly puckered, as reflected by the internal sum of bond angles (ring of ligand 1 ~ 704.6°, where 720° is expected for a hexagon).

The Al–O bond lengths are shorter than the Al–N bond lengths. This difference is caused by the smaller radius of the oxygen atoms and its larger ionic contribution to the Al–O bond. As evidenced by the pattern of bond lengths, the chelate rings are delocalised (O(1)–C(1): 1.2932(15) Å, C(1)–C(2): 1.3702(18) Å, C(2)–C(3): 1.4245(18) Å, N(1)–C(3): 1.3082(17) Å). Compared with the free β-ketoimine ligand, there is lengthening of the O(1)–C(1) and C(2)–C(3) bonds and a shortening of the N(1)–C(3) bond, as the bonds gain less and more double bond character, respectively.[54]

Bond lengths among the three ligands in the complex vary only slightly and, in most cases, are within three estimated standard deviations of one another and, hence, are crystallographically identical. The only notable bond length difference between ligands include O–C and N–C backbone bond lengths, which are crystallographically identical only for two of the ligands, but different for the O(3) and N(3) containing ligand, most likely due to both heteroatoms on this ligand binding to the Al in equatorial positions. Bond angles within the ligand are less similar when comparing the three chelates, most often not falling within three estimated standard deviations of one another. One example is the bond angle of the methine environment, which varies from 123.33(11)–125.38(12) Å across the three ligands. Complexes described in this contribution feature very similar crystallographic observations and, as such, ligand specific bond lengths and angles will not be further discussed for the ensuing examples, but their crystal structures can be found in Figure 3.

In addition to SCXRD characterisation, compound **1** was also identified *via* ^{1}H, ^{13}C{^{1}H} NMR (with aid of 2D spectra), MS and EA. The ^{1}H NMR spectrum does not show any resonances for the NH proton of the free β-ketoiminate ligand, and the peaks are shifted from the uncomplexed compound. Interestingly, **1** shows a complicated NMR, with most methyl groups showing different resonances as well as there being three different methine environments in both ^{1}H and ^{13}C{^{1}H} NMR spectra, attributable to the aforementioned *mer*-geometry. Due to different *cis* and *trans* heteroatomic relationships across the aluminium metal and varying amounts of steric encumbrance, no proton or carbon environment across the three ligands is the same and, hence, the corresponding peaks are slightly shifted from one another. This phenomenon is most clearly illustrated by the presence of three C*H* peaks in the ^{1}H NMR at 5.03, 4.97 and 4.87 ppm, in a 1:1:1 ratio. Methine protons are followed by two singlet peaks, that lost doublet character due to loss of enamino proton upon complexation, at 2.92 and 2.79 ppm corresponding to the N-substituent CH_3 groups in a 1:2 ratio. It is important to note that only two peaks are observed in this region, and they correspond to the two environments intrinsic to the *mer* conformation (two methyl imino groups *trans* to one another and one Me–N *trans* to O). Finally, there are six methyl groups, three corresponding to the CH_3CO groups (1.99, 1.93, 1.90 ppm) and three corresponding to the CH_3CN groups (1.59, 1.56, 1.55 ppm), each integrating to 3 protons. As expected, ^{13}C{^{1}H} NMR environments also split into three for each of the ligands and are consistent with the formation of **1**.

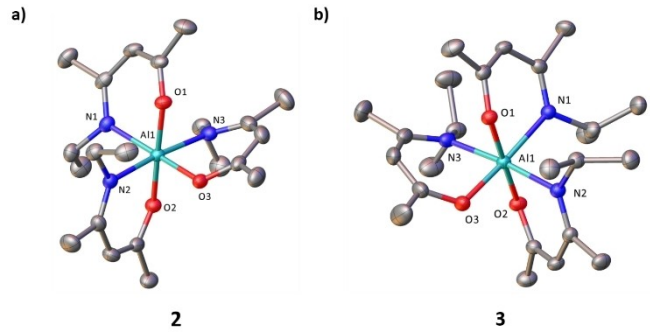

Figure 3. Molecular structures of (a) **[Al(Et-acnac)$_3$]** (**2**) and (b) **[Al(^{i}Pr-acnac)$_3$]** (**3**) Hydrogen atoms omitted for clarity.

[Al(MeCN(Et)CHC=OMe)$_3$] ([Al(Et-acnac)$_3$], 2)

Compound **2**, **[Al(Et-acnac)$_3$]**, was synthesised by the same procedure as the methyl analogue, with white crystals precipitated from a concentrated diethyl ether solution at −20 °C, in excellent purity and in good yield (64 %). The crystal structure of compound **2** was determined *via* SCXRD and it crystallises in the higher symmetry monoclinic space group $P2_1/n$ (Figure 3a). Three bidentate ligands bind to the metal in the same manner as with compound **1** (R = Me).

Complex **2** is also in a distorted octahedral geometry in *mer*-configuration, with most distortions in the ethyl analogue being similar to those of the methyl. The N(1)–Al(1)–N(3) angle, however, shows more distortion in **2**, with a 95.82(4)° angle (91.56(4)° in **1**). This can be understood based on the fact that as the alkyl substituents on N(1) and N(3) are closest together in **2**, they have to span out into the same plane, hence distorting further away from the 90° optimum geometry. As with complex **1**, **2** also crystalizes as a racemic mixture of the enantiomers lambda and delta.

The Al–O bond lengths are slightly shorter than in the methyl analogue (1.8512(9)–1.8693(9) Å) while the Al–N bond lengths are slightly larger (2.0441(10)–2.0498(10) Å). These findings can be rationalised by the added steric bulk of the ethyl group at the N atoms, therefore forcing them to bind further away from the Al atom, resulting in the O atoms binding closer to supply the Al atom with sufficient electron density, in combination with the delocalised nature of β-ketoiminate ligands. The O(1)–C(1) and N(1)–C(3) bond lengths for the ethyl analogue are very similar to that of the methyl complex (O(1)–C(1) 1.2932(15) Å in **1** and 1.2968(15) in **2**; N(1)–C(3) 1.3082(17) in **1** and 1.3123(16) in **2**). The N(1)–C(6) bond length in the ethyl complex **2** is larger compared to that of the methyl analogue (**1**), with bond lengths of 1.4764(16) and 1.4685(16) Å, respectively. This longer N(1)–C(6) bond length in **2** can be attributed to the increased steric strain imposed by the ethyl groups in each ligand, forcing them to contort further away from the ligand backbone. As with **1**, there are similar trends in differences in bond lengths and angles between each of the three chelating ligands in **2**.

The ^{1}H NMR spectrum of **2** does not show any resonances for the NH proton of the free β-ketoimine ligand, peaks are shifted, and there is loss of multiplicity due to the removal of the enamino proton upon complexation. As with the methyl analogue, **2** also has complicated NMR spectra. All methyl, methylene and methine groups have different chemical shifts in the ^{1}H and ^{13}C{^{1}H} NMR spectra due to the *mer*-geometry of the complex. The most downfield environments are the methine groups on the ligand backbone occurring at 5.00, 4.96 and 4.88 ppm, followed by the methylene groups of the ethyl N-substituents between 3.40–3.19 ppm, while the methyl groups on the ethyl groups are upfield shifted to 1.27, 1.21 and 1.06 ppm. ^{13}C{^{1}H} NMR environments are also consistent with the formation of **2**.

[Al(MeCN(ⁱPr)CHC=OMe)₃] ([Al(ⁱPr-acnac)₃], 3)

Compound **3**, **[Al(ⁱPr-acnac)$_3$]**, was synthesised analogously to **1** and **2**, with white crystals precipitated from a concentrated diethyl ether solution at −20 °C, in excellent purity and good yield (61 %). The crystal structure of **3** was determined *via* SCXRD and it showed that it crystallises in the triclinic space group $P\bar{1}$ (Figure 3b). Three bidentate ligands bind to the metal atom in the same manner as with the other tris(β-ketoiminate) aluminium compounds, **1** and **2**, described so far.

Complex **3** also adopts a distorted octahedral geometry as the *mer*-stereoisomer. Overall, the isopropyl complex is more distorted than the ethyl analogue due to the added steric bulk of the N-substituent, which is evident by a larger distortion in the ligand pincer bonding angle, O(1)–Al(1)–N(1), of 87.34(4)°, compared to 88.10(4)° in **2**. Distortions of the O(1)–Al(1)–N(1), O(1)–Al(1)–O(2) and N(1)–Al(1)–O(3) bond angles of 87.34(4), 177.27(4) and 174.38(5)° respectively, are generally greater than those reported in the literature,[20,26,27] indicating that the isopropyl groups impose a greater steric bulk closer the metal, therefore creating a larger distortion. As with complexes **1** and **2, 3** also crystalizes as a racemic mixture of the enantiomers lambda and delta.

As expected, with the increase in steric bulk on going from ethyl to isopropyl N-substituents, there is an increase in Al–N bond lengths (2.0529(12)–2.0638(11) Å), while changes in Al–O bond lengths are negligible (1.8445(9)–1.8742(9) Å). The N-(1)–C(3) and N(1)–C(6) bond lengths are longer in **3** due to the increased bulk of the alkyl group. The Al-heteroatom bonds found in this compound are in good agreement with those found in Jana's aryl *tris*-phenyl-β-ketoiminate aluminium complex (Al–O: 1.839(1)–1.865(1) Å, Al–N: 2.040(2)–2.062(2)), Olejník's methoxyaryl (Al–O:1.8276(16)–1.8680(16) Å, Al–N: 2.0511(19)–2.0723(19)), and Altaf's *tert*-butylphenyl complexes (Al–O: 1.8321(9)–1.8764 (10) Å, Al–N: 2.0403(11)–2.0671(11)).[20,26,27] It is interesting to note that, although one could assume that the isopropyl groups in **3** would cause less steric encumbering between ligands than the aryl groups, it seems this is not the case as **3** has slightly longer Al–O and Al–N bond lengths in order to reduce clashing of ligands. As with complexes **1** and **2**, **3** exhibits similar trends in differences in bond lengths and angles among each of the three chelating ligands.

Compound **3** was also identified *via* ^{1}H, ^{13}C{^{1}H} NMR, MS and EA. Similarly to **1** and **2**, the ^{1}H NMR spectrum of **3** does not show any resonances for the NH proton of the free β-ketoimine compound, the peaks are shifted relative to the free ligand and there is loss of multiplicity due to the removal of the enamino proton upon complexation. As with the other alkyl analogues, **3** shows a complicated NMR, with all methyl, methylene and methine groups displaying different resonances in the ^{1}H and ^{13}C{^{1}H} NMR spectra, due to the *mer*-geometry of the complex.

[Al(MeCN(Ph)CHC=OMe)₃] ([Al(Ph-acnac)₃], 4)

Compound **4**, **[Al(Ph-acnac)$_3$]**, was synthesised by the same procedure as the other analogues and according to the literature,[20] with white crystals precipitated from a concentrated toluene solution at −20 °C in excellent purity and good yield (65 %). The crystal structure of compound **4** was determined *via* SCXRD, with bond lengths and angles occurring within three standard deviations with when compared to Jana's report.[20] Three bidentate ligands bind to the metal in a distorted octahedral geometry with *mer*-stereoisomerism as seen for compounds **1**–**3.** As with complexes **1**–**3** and, in accordance with the original report of Jana, **4** also crystalizes as a racemic mixture of the enantiomers lambda and delta. The formation of compound **4** was also confirmed by ^{1}H, ^{13}C{^{1}H} NMR (with aid of 2D spectra), MS and EA and is in good agreement with the literature[20] and with the previous examples described thus far.

[Al(MeCN(Mes)CHC=OMe)₃] (where Mes=2,4,6-trimethylphenyl ([Al(Mes-acnac)₃], 5)

Compound **5**, **[Al(Mes-acnac)$_3$]**, was synthesised in an analogous manner to **1**–**4**, with white crystals precipitated from a concentrated toluene solution at −20 °C in excellent purity and moderate yield (47 %). Despite numerous attempts, no adequate single crystals could be obtained of compound **5** and they could only be refined by a model with a high R-factor (14.35 %). This appears to be a feature of the crystal growth, since multiple attempts yielded the same high mosaicity in the collected frames.

Due to the poor quality of the data, crystal symmetry, bonds lengths and angles will not be discussed at great length and will only be used as guidance to assist observations in the TGA data (*via* trends). Nevertheless, this pseudo-crystallographic model, shown in Figure 4, does provide key information, which would have been very difficult to elucidate without it. Due to the large steric bulk of the mesityl (2,4,6-trimethylphenyl) R group in the ligand used to synthesise complex **5**, it is no longer possible to accommodate three β-ketoimine ligands binding in a bidentate mode around the metal to form a six-coordinate octahedral geometry. Instead, only a five-coordinate trigonal bipyramidal geometry can be formed, with axial O-

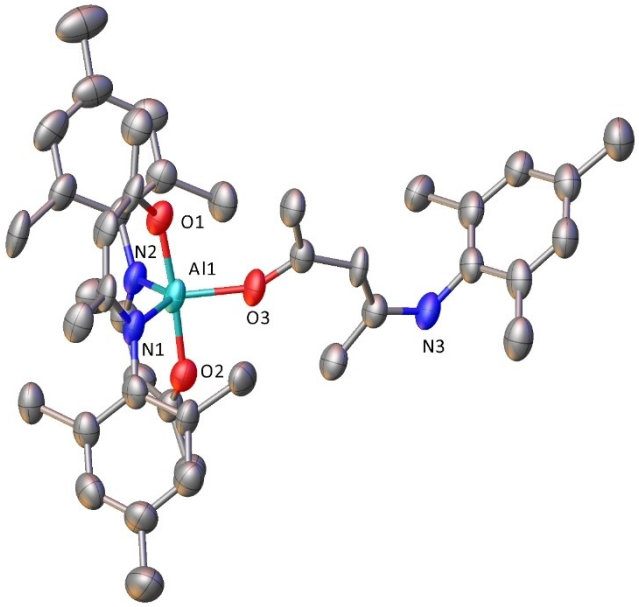

Figure 4. Molecular structure of [**Al(Mes-acnac)$_3$**] (**5**). Thermal ellipsoids are pictured at 50% probability. Hydrogen atoms are omitted for clarity.

binding of two chelating ligands and one ligand only binding in a monodentate mode (Figure). Intuitively, the monodentate β-ketoiminate binds to the Al through the oxygen atom, most likely owing to steric factors, as the ligand is positioned as such that the bulky mesityl group is situated as further away as possible from the crowded complex centre. Furthermore, aluminium also has a high affinity to oxygen, making this bonding motif also supported by electronic factors. As such, these findings suggest that the limit to steric saturation has been reached when R = Mes, forcing the metal complex to go from six- to five-coordinate.

In addition to SCXRD characterisation, compound **5** was also identified *via* ^{1}H, ^{13}C{^{1}H} NMR (with aid of 2D spectra), MS and EA. ^{1}H and ^{13}C{^{1}H} NMR spectrum is consistent with complexation and with the spectra of the other species **1**–**4** described so far.

Comparison of crystal structures

Table 1 shows a comparison of the Al–O and Al–N bond lengths as well as the O–Al–N ligand pincer angles found in each of the novel complexes, in addition to Jana's structure.[20]

Table 1. Comparison of the Al–O and Al–N bond lengths and the O–Al–N pincer angles for complexes **1**–**4** (the specific N-substituent of the ligand used in each complex is indicated in parentheses for clarity).

	Al–O [Å]	Al–N [Å]	O–Al–N [°]
1 (Me)	1.859–1.877	2.031–2.035	88.73–90.30
2 (Et)	1.851–1.869	2.044–2.049	88.10–90.56
3 (^{i}Pr)	1.845–1.874	2.053–2.064	87.34–89.89
4 (Ph)[20]	1.839–1.865	2.040–2.062	88.09–90.54

For the *tris* bidentate complexes (R = Me, Et, ^{i}Pr and Ph), there is a general trend of increasing Al–N bond length with varying steric bulk of the R group (^{i}Pr being the bulkiest). The effects of hyperconjugation do not play a key role in determining the Al–N bond lengths among differing N-substituents as shorter bond lengths for longer, more branched alkyl chains, are not observed. The lengthening of the Al–N bond is generally accompanied by a shortening of the Al–O bond although that is not the case for the ^{i}Pr analogue, most likely to prevent greater steric clash with adjacent imino groups on other ligands if the O atoms were to be pulled in more closely.

Trends in the O–Al–N ligand pincer angles are less clear, however the less crowded 5-coordinate mesityl complex is less strained as it is not 6-coordinate like **1**–**4**. Further evidence that the ^{i}Pr complex, **3**, is the most sterically encumbered complex out of all the octahedral adducts can be noted by the fact that is has the smallest ligand pincer angle out of the four complexes.

Deposition Numbers 2211016-2211018 for **1**–**3** contain the supplementary crystallographic data for this paper. These data are provided free of charge by the joint Cambridge Crystallographic Data Centre and Fachinformationszentrum Karlsruhe Access Structures service.

Accessing the Al complexes suitability as precursors

Thermal decomposition analysis of the tris(β-ketoimine) aluminium complexes 1–5

Thermal analysis of the precursors allows for an initial assessment of the suitability of the tris(β-ketoiminate) aluminium complexes, **1**–**5**, as precursors for the deposition of aluminium metal or aluminium oxide via a deposition technique of choice. All β-ketoimine compounds described herein fully decompose (*i.e.* 100% mass loss of ligand weight fraction).

Thermal decomposition summary

Figure 5a shows the overlapping thermograms of complexes **1**–**5**, with derivatives highlighting the onset of thermal degradation steps shown in Figure 5b. The TGA analyses indicate that, from the five tris(β-ketoiminate) aluminium complexes described in this work, the two smaller alkyl complexes, **1** and **2**, degrade through a single thermal event which is initiated within the desired temperature bracket of 50–200 °C, indicating that deposition onto low-cost flexible materials is feasible. Compound **1** (R = Me) exhibits very promising features, with low decomposition temperature, with mass loss beginning at 152 °C, and suggesting decomposition into Al metal rather than complete degradation to Al_2O_3.

Complexes **2**–**5** exhibit mass losses consistent with the formation of Al_2O_3. The complexes containing aromatic rings, **4** and **5**, degrade in multiple steps, with the final decomposition event initiating above 250 °C, while the sterically hindered aliphatic ^{i}Pr-substituted β-ketoimine complex, **3**, shows an

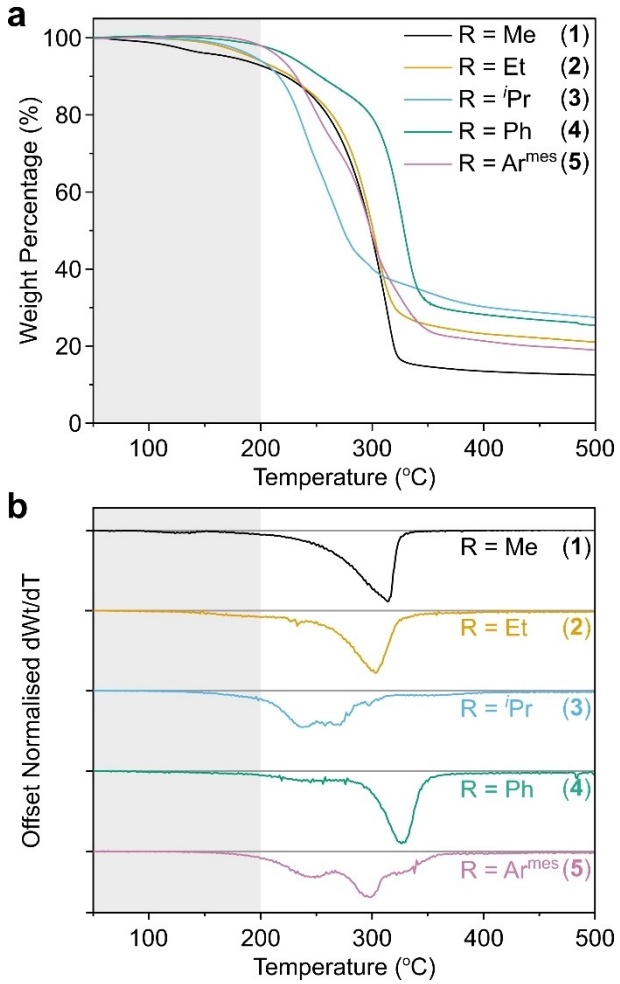

Figure 5. (a) Overlapping thermograms of the tris(β-ketoiminate) aluminium complexes **1**–**5**. (b) Offset derivatives of thermograms, with $dWt/dT = 0$ for each curve given as a grey line to guide the eye. Grey background given between 50–200 °C to highlight desired decomposition window. Individual thermograms provided in ESI. Curve colours taken from reference [42],[56] to maximise contrast for readers with prot/deuteranopia.

intermediate behaviour, with multiple overlapping degradations likely initiating beyond the upper bracket limit of 200 °C. While the decomposition temperature of **3** is promising, the mass loss is less than satisfactory, producing either aluminium metal or aluminium oxide films with considerable carbon contamination. Compound **3** likely decomposes at lower temperatures than the other octaheadral analogues due to the isopropyl N-substituents being the bulkiest among the six-coordinated complexes and, as such, yielding a more distorted octaheadral geometry around the metal, so it requires less energy for decomposition.[55] Accordingly, while complexes **3**–**5** are good candidates as precursors for the deposition of aluminium oxide, they are not suitable for depositions onto temperature sensitive substrates.

Pyrolysis of tris(β-ketoiminate) aluminium complexes

Residues after TGA could not be analysed by techniques such EA, XRD and XPS to further probe their composition as the TGA machines used exposed samples to atmospheric conditions after measurement, which would oxidise any Al(0) residue formed during the thermal degradation. To confirm whether each precursor decomposed to aluminium metal under inert conditions, inert furnace heating experiments (pyrolysis) were undertaken. Two precursors were chosen for initial experiments: **[Al(Et-acnac)$_3$]** (**2**), a single-component, low temperature-degradation aliphatic complex, and **[Al(Ph-acnac)$_3$]** (**4**), a two-component, high temperature-degradation aromatic complex. Initially, 0.15 g of each compound was loaded into a crucible in a tube furnace under a flow of N_2 and heated to 350, 400 and 500 °C in subsequent experiments. Brown powdery deposits were not conductive and PXRD analysis revealed amorphous material. Since Al_2O_3 is not crystalline when formed at temperatures below 900 °C, it was not detected in the XRD pattern. Repeat experiments under vacuum yielded identical results.

AACVD of Al_2O_3

A proof of concept study was undertaken to validate the precursors potential to deposit Al_2O_3 via AACVD using a solution of **1** in toluene. Thin films of Al_2O_3 were deposited onto glass slides inside a tube furnace set to 450 °C. The aerosol containing the precursor was transported through the tube furnace with a carrier gas of N_2 with a flow rate of 1 Lmin^{-1}. Films were transparent and well adhered to the substrate and could only be removed with abrasion from a steel stylus. EDX of the films confirmed the Al content (73.8 at.% Al, 13.6 at.% C) and SEM showed films to be smooth and relatively featureless, with some areas of nucleation (Figure 6), presumably the beginnings of the next layer growth, indicative of island growth mechanism. Formation of any carbides or nitrides was ruled out by XRD, which did not detect any crystalline material.

To confirm the formation of Al_2O_3, X-ray photoelectron spectroscopy (XPS) was carried out on samples deposited at 450 °C (Figure 6). The small doublet splitting (0.42 eV) of the Al $2p_{3/2}$ and the Al $2p_{1/2}$ renders fitting of the data unreliable, therefore raw data is presented as an alternative (after calibration to adventitious C 1s at 285 eV). As expected, the binding energy of Al 2p was in the region of 73.7 eV, in line with previously reported XPS for Al_2O_3.[57–62]

Conclusions

We described the synthesis and characterisation of four novel tris(β-ketoiminate) Al(III) complexes, including the first examples where the N-substituent is an alkyl group, complexes **1**–**3**. N-Substituents with varying sizes were chosen as part of a comprehensive evaluation of their effect on the resulting structure of the complex and, consequently, their decomposition profile. Most Al complexes described in this work adopt a

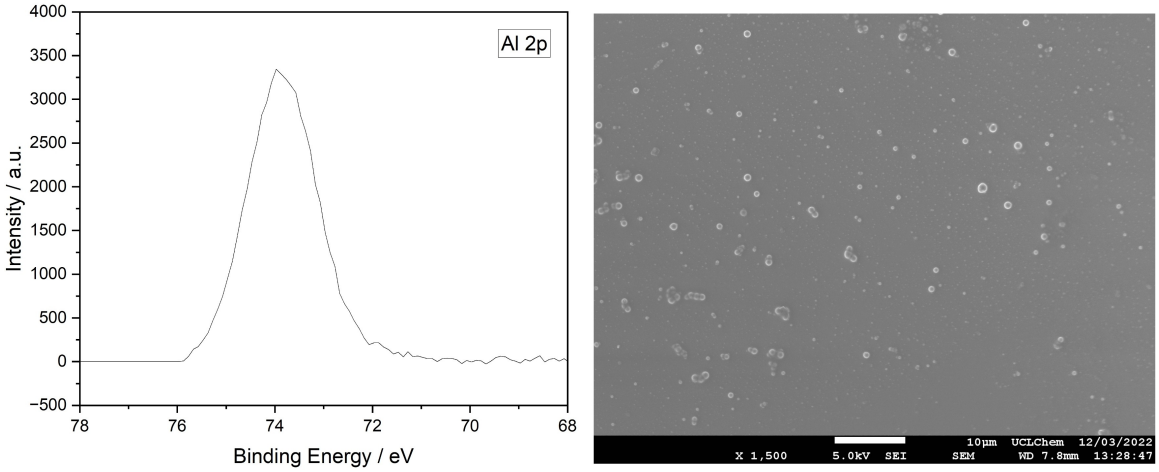

Figure 6. XPS (left) and SEM (right) evidence of the formation of Al_2O_3 thin films grown on glass substrates via AACVD from a toluene solution of **1** at 450 °C, with a 1 $Lmin^{-1}$ flow rate of N_2 carrier gas. Scale bar on SEM represents 10 μm.

distorted octahedral arrangement around the aluminium site, form the *mer*-isomer and crystalizes as a racemic mixture of the enantiomers Δ and Λ. The exception is **5** (R = Mes), which exhibits a trigonal bipyramidal configuration, with two ligands in bidentate mode and one monodentate, bound to the aluminium via the oxygen atom, as a consequence of the bulkier nature of the Mes-acnac β-ketoiminate ligand. Compound **5** is the only complex of this niche motif, and it signifies the steric limit at which three β-ketoiminate ligands, with bulky N-substituents, can no longer all bind in a bidentate mode around the metal.

The decomposition profile of all complexes have been studied *via* TGA and their suitability as metal-organic decomposition (MOD) precursors was evaluated. Compounds **1**–**5** generally showed good decomposition properties, with the best precursor being **[Al(Me-acnac)$_3$]** (**1**), displaying excellent mass loss properties and a low onset decomposition temperature (< 200 °C). These compounds could have potential as precursors for a range of deposition techniques, including MOCVD and, since they are highly soluble in a range of organic solvents, it is hypothesised that they may be particularly applicable in solution-based techniques such as AACVD and inkjet printing.

Acknowledgments

The EPSRC are thanked for funding this work (EP/V027611/1). AJC thanks the Ramsay Memorial Trust for funding.

Conflict of Interest

The authors declare no conflict of interest.

Data Availability Statement

The data that support the findings of this study are available from the corresponding author upon reasonable request.

Keywords: aluminium · β-ketoiminate · deposition · precursors · thin films

[1] R. C. Mehrotra, *Pure Appl. Chem.* **1988**, *60*, 1349–1356.
[2] R. H. Holm, G. W. Everett, A. Chakravorty, *Progress in Inorganic Chemistry*, John Wiley & Sons, **1966**.
[3] L. Bourget-Merle, M. F. Lappert, J. R. Severn, *Chem. Rev.* **2002**, *102*, 3031–3065.
[4] C. E. Knapp, C. J. Carmalt, *Chem. Soc. Rev.* **2016**, *45*, 1036–1064.
[5] C. E. Knapp, P. Marchand, C. Dyer, I. P. Parkin, C. J. Carmalt, *New J. Chem.* **2015**, *39*, 6585–6592.
[6] C. E. Knapp, C. Dyer, N. P. Chadwick, R. Hazael, C. J. Carmalt, *Polyhedron* **2018**, *140*, 35–41.
[7] Y. Yang, H. Li, C. Wang, H. W. Roesky, *Inorg. Chem.* **2012**, *51*, 2204–2211.
[8] P.-C. Kuo, I.-C. Chen, J.-C. Chang, M.-T. Lee, C.-H. Hu, C.-H. Hung, H. M. Lee, J.-H. Huang, *Eur. J. Inorg. Chem.* **2004**, *2004*, 4898–4906.
[9] C. Pflitsch, A. Muhsin, U. Bergmann, B. Atakan, *Surf. Coat. Technol.* **2006**, *201*, 73–81.
[10] M. P. Singh, S. A. Shivashankar, *Surf. Coat. Technol.* **2002**, *161*, 135–143.
[11] A. Devi, S. A. Shivashankar, A. G. Samuelson, *J. Phys. IV* **2002**, *12*, 139–146.
[12] T. Maruyama, S. Arai, *Appl. Phys. Lett.* **1992**, *60*, 322.
[13] J. S. Kim, H. A. Marzouk, P. J. Reucroft, J. D. Robertson, C. E. Hamrin, *Appl. Phys. Lett.* **1998**, *62*, 681.
[14] M. A. Bhide, J. A. Manzi, C. E. Knapp, C. J. Carmalt, *Molecules* **2021**, *26*, 3165.
[15] D. Pugh, P. Marchand, I. P. Parkin, C. J. Carmalt, *Inorg. Chem.* **2012**, *51*, 6385–6395.
[16] S. J. W. Cummins, H. P. Fraser, J. R. Fulton, M. P. Coles, C. M. Fitchett, S. J. W. Cummins, H. P. Fraser, J. R. Fulton, M. P. Coles, C. M. Fitchett, *Aust. J. Chem.* **2015**, *68*, 641–647.
[17] P. Shukla, J. C. Gordon, A. H. Cowley, J. N. Jones, *J. Organomet. Chem.* **2005**, *690*, 1366–1371.
[18] P. C. Kuo, I. C. Chen, H. M. Lee, C. H. Hung, J. H. Huang, *Inorg. Chim. Acta* **2005**, *358*, 3761–3767.
[19] A. Z. Bradley, D. L. Thorn, G. V. Glover, *J. Org. Chem.* **2008**, *73*, 8673–8674.
[20] B. Jana, W. Uhl, *Inorg. Chim. Acta* **2017**, *455*, 61–69.
[21] T. Proll, W. Walter, *Chem. Ber.* **1983**, *116*, 1564–1572.

[22] C. E. Knapp, G. Hyett, I. P. Parkin, C. J. Carmalt, *Chem. Mater.* **2011**, *23*, 1719–1726.
[23] P. Steiniger, D. Dittrich, C. Scheiper, C. John, C. Wölper, S. Schulz, *Z. Anorg. Allg. Chem.* **2018**, *644*, 1367–1375.
[24] R. C. Yu, C. H. Hung, J. H. Huang, H. Y. Lee, J. T. Chen, *Inorg. Chem.* **2002**, *41*, 6450–6455.
[25] M. Bouyahyi, T. Roisnel, J. F. Carpentier, *Organometallics* **2010**, *29*, 491–500.
[26] C. T. Altaf, H. Wang, M. Keram, Y. Yang, H. Ma, *Polyhedron* **2014**, *81*, 11–20.
[27] R. Olejník, J. Bažantová, Z. Růžičková, J. Merna, Z. Hošálek, A. Růžička, *Inorg. Chem. Commun.* **2015**, *55*, 161–164.
[28] A. C. Jones, H. C. Aspinall, P. R. Chalker, *Chemical Vapour Deposition: Precursors, Processes and Applications*, RSC Publishing, **2008**.
[29] J. Von Hoene, R. G. Charles, W. M. Hickam, *J. Phys. Chem.* **1958**, *62*, 1098–1101.
[30] X. Hu, J. Schuster, S. E. Schulz, T. Gessner, *Phys. Chem. Chem. Phys.* **2015**, *17*, 26892–26902.
[31] J. A. Manzi, C. E. Knapp, I. P. Parkin, C. J. Carmalt, *Eur. J. Inorg. Chem.* **2015**, *2015*, 3658–3665.
[32] L. A. Ryabova, Y. S. Savitskaya, *Thin Solid Films* **1968**, *2*, 141–148.
[33] S. P. Douglas, S. Mrig, C. E. Knapp, *Chem. Eur. J.* **2021**, *27*, 8062–8081.
[34] S. P. Douglas, C. E. Knapp, *ACS Appl. Mater. Interfaces* **2020**, *12*, 26193–26199.
[35] S. J. A. Moniz, C. S. Blackman, C. J. Carmalt, G. Hyett, *J. Mater. Chem.* **2010**, *20*, 7881–7886.
[36] A. W. Coats, J. P. Redfern, *Analyst* **1963**, *88*, 906–924.
[37] D. H. Lee, S. E. Park, K. Cho, Y. Kim, T. Athar, I. M. Lee, *Tetrahedron Lett.* **2007**, *48*, 8281–8284.
[38] D. Bahulayan, S. K. Das, J. Iqbal, *J. Org. Chem.* **2003**, *68*, 5735–5738.
[39] S. Gogoi, R. Bhuyan, N. C. Barua, *Synth. Commun.* **2005**, *35*, 2811–2818.
[40] B. Govindh, B. S. Diwakar, Y. L. N. Murthy, *Org. Commun.* **2012**, *5:3*, 105–119.
[41] H. M. Lee, J. Y. Seo, A. Jung, S.-Y. Y. Choi, S. H. Ko, J. Jo, S. Bin Park, D. Park, *ACS Appl. Mater. Interfaces* **2014**, *6*, 15480–15487.
[42] W. L. Gladfelter, D. C. Boyd, K. F. Jensen, *Chem. Mater.* **1989**, *1*, 339–343.
[43] T. H. Baum, C. E. Larson, R. L. Jackson, *Appl. Phys. Lett.* **1998**, *55*, 1264.
[44] M. Das, D. T. Haworth, J. W. Beery, *Inorg. Chim. Acta* **1981**, *49*, 17–20.
[45] M. Kuhn, N. Fuchs, S. Steimann, *Eur. J. Inorg. Chem.* **2000**, *2001*, 359–361.
[46] W. A. E. Omar, *J. Adv. Res.* **2013**, *4*, 525–529.
[47] W. A. E. Omar, H. Haverinen, O. E. O. Hormi, *Tetrahedron* **2009**, *65*, 9707–9712.
[48] N. Johansson, T. Osada, S. Stafström, W. R. Salaneck, V. Parente, D. A. Dos Santos, X. Crispin, J. L. Brédas, *J. Chem. Phys.* **1999**, *111*, 2157.
[49] M. Muccini, M. A. Loi, K. Kenevey, R. Zamboni, N. Masciocchi, A. Sironi, *Adv. Mater.* **2004**, *16*, 861–864.
[50] C. F. R. A. C. Lima, R. J. S. Taveira, J. C. S. Costa, A. M. Fernandes, A. Melo, A. M. S. Silva, L. M. N. B. F. Santos, *Phys. Chem. Chem. Phys.* **2016**, *18*, 16555–16565.
[51] T. B. Tai, L. Cao, F. Mattelaer, G. Rampelberg, F. S. M. Hashemi, J. Dendooven, J. R. Van Ommen, C. Detavernier, M. F. Reyniers, *J. Phys. Chem. C* **2019**, *123*, 485–494.
[52] F. S. M. Hashemi, L. Cao, F. Mattelaer, T. Sajavaara, J. R. van Ommen, C. Detavernier, *J. Vac. Sci. Technol. A: Vacuum, Surfaces, and Films* **2019**, *37*, 040901.
[53] A. Saini, S. K. Jat, D. S. Shekhawat, A. Kumar, V. Dhayal, D. C. Agarwal, *Mater. Res. Bull.* **2017**, *93*, 373–380.
[54] G. I. Zharkova, P. A. Stabnikov, I. A. Baidina, A. I. Smolentsev, S. V. Tkachev, *Polyhedron* **2009**, *28*, 2307–2312.
[55] M. A. Bhide, K. L. Mears, C. C. Carmalt, C. E. Knapp, *Nanomaterials via Single-Source Precursors: Synthesis, Processing and Applications*, Elsevier, **2022** .
[56] B. Wong, *Nat. Methods* **2011**, *8*, 441.
[57] H. E. Evans, W. M. Bowser, W. H. Weinberg, *Appl. Surf. Sci.* **1980**, *5*, 258–274.
[58] S. Lars, T. Andersson, M. S. Scurrell, *J. Catal.* **1979**, *59*, 340–356.
[59] J. F. Moulder, W. F. Stickle, P. E. Sobol, K. D. Bomben, *Handbook of X-Ray Photoelectron Spectroscopy*, Perkin-Elmer Corporation, **1992**.
[60] S. Ben Amor, G. Baud, M. Jacquet, G. Nansé, P. Fioux, M. Nardin, *Appl. Surf. Sci.* **2000**, *153*, 172–183.
[61] S. Wannaparhun, S. Seal, V. Desai, *Appl. Surf. Sci.* **2002**, *185*, 183–196.
[62] G. Spina, B. Bonelli, P. Palmero, L. Montanaro, *Mater. Chem. Phys.* **2013**, *143*, 286–295.

Manuscript received: November 15, 2022
Revised manuscript received: December 22, 2022
Accepted manuscript online: December 22, 2022